Molecular immunology and signaling

Basic

Research Article

Distinct modulation of cellular immunopeptidome by the allosteric regulatory site of ER aminopeptidase 1

Ioannis Temponeras[1,2], Martina Samiotaki[3], Despoina Koumantou[1], Martha Nikopaschou[1,4], Jonas J.W. Kuiper[5,6], George Panayotou[3] and Efstratios Stratikos[1,4] (ID)

[1] National Centre for Scientific Research Demokritos, Agia Paraskevi, Greece

[2] Department of Pharmacy, University of Patras, Patra, Greece

[3] Biomedical Sciences Research Center "Alexander Fleming," Institute for Bioinnovation, Vari, Greece

[4] Department of Chemistry, National and Kapodistrian University of Athens, Zografou, Greece

[5] Department of Ophthalmology, University Medical Center Utrecht, Utrecht University, Utrecht, The Netherlands

[6] Center for Translational Immunology, University Medical Center Utrecht, Utrecht University, Utrecht, The Netherlands

ER aminopeptidase 1 (ERAP1) is an ER-resident aminopeptidase that excises N-terminal residues of peptides that then bind onto Major Histocompatibility Complex I molecules (MHC-I) and indirectly modulates adaptive immune responses. ERAP1 contains an allosteric regulatory site that accommodates the C-terminus of at least some peptide substrates, raising questions about its exact influence on antigen presentation and the potential of allosteric inhibition for cancer immunotherapy. We used an inhibitor that targets this regulatory site to study its effect on the immunopeptidome of a human cancer cell line. The immunopeptidomes of allosterically inhibited and ERAP1 KO cells contain high-affinity peptides with sequence motifs consistent with the cellular HLA class I haplotypes but are strikingly different in peptide composition. Compared to KO cells, allosteric inhibition did not affect the length distribution of peptides and skewed the peptide repertoire both in terms of sequence motifs and HLA allele utilization, indicating significant mechanistic differences between the two ways of disrupting ERAP1 function. These findings suggest that the regulatory site of ERAP1 plays distinct roles in antigenic peptide selection, which should be taken into consideration when designing therapeutic interventions targeting the cancer immunopeptidome.

🖥 Additional supporting information may be found online in the Supporting Information section at the end of the article.

Introduction

Adaptive immune responses mediated by the interaction between T cells and APCs are controlled by the presentation of small

Correspondence: Dr. Efstratios Stratikos
e-mail: estratikos@chem.uoa.gr

antigenic fragments (peptides) bound onto proteins of the MHC [1]. MHC class I proteins (MHC-I) present short peptides that are generated from intracellular proteins by complex proteolytic pathways [2]. The sum of peptides presented on the cell surface bound onto MHC class I proteins is termed the class I cellular immunopeptidome and is a major marker of cellular health [3]. Changes in the cellular immunopeptidome can signify that the cell is infected by a pathogen or transformed. These changes can be detected by cytotoxic CD8$^+$ T lymphocytes, which proceed to kill the infected cell [4]. Due to the importance of the immunopeptidome, several efforts are underway to help understand its exact role in disease and to manipulate its contents for therapeutic applications such as in cancer immunotherapy or MHC-I-associated inflammatory autoimmunity [5].

Peptides presented by MHC-I are often initially generated by the proteolytic action of the proteasome on protein antigens. A subset of the peptide products of the proteasome are transferred to the ER by the action of a specialized transporter [6]. Some of the peptides that enter the ER are of suitable length and sequence to bind onto nascent MHC-I with the aid of a multiprotein complex of chaperones called the peptide loading complex [7]. Some peptides, however, are too long to bind to MHC-I, which has strong preferences for length [8]. These elongated antigenic peptide precursors are trimmed by two ER-resident aminopeptidases, the best-characterized one being ER aminopeptidase 1 (ERAP1) [2]. Thus, ERAP1 is important for generating many antigenic peptides but at the same time can also over-trim some peptides to lengths too short to bind onto MHC-I, essentially destroying their chances of being presented on the cell surface [9]. This way, ERAP1 can influence the cellular immunopeptidome and regulate adaptive immune responses. Indeed, most of the associations between ERAP1 activity and predisposition to autoimmunity or responses to cancer immunotherapy are considered to be mediated through its effects on the immunopeptidome [10, 11]. ERAP1 can recognize determinants throughout the peptide substrate sequence with significant sequence degeneracy, which is, however still poorly understood [12]. The *ERAP1* gene is highly polymorphic and encodes a variety of enzyme allotypes implicated in human diseases due to their diverse enzymatic specificities and activities [13]. Accordingly, human populations may benefit from the functional variation of ERAP1 through enhanced flexibility and breadth of their immune responses [14]. Due to its roles in antigen processing, ERAP1 is currently an emerging target for cancer immunotherapy and HLA-associated autoimmunity [15, 16]. Several inhibitors have been developed [17], including inhibitors that target allosteric sites with enhanced selectivity [18–21], although no clinical results have been reported yet.

ERAP1 trims peptides by a complex mechanism that involves a large conformational change that cyclically exposes or sequesters a large internal cavity from the external solvent [22]. The closed conformation is more catalytically active, while the open conformation is necessary for capturing longer peptides [23, 24]. Catalytical cleavage of the *N*-terminus of a peptide takes place in the active site located at one edge of the internal cavity. Interactions
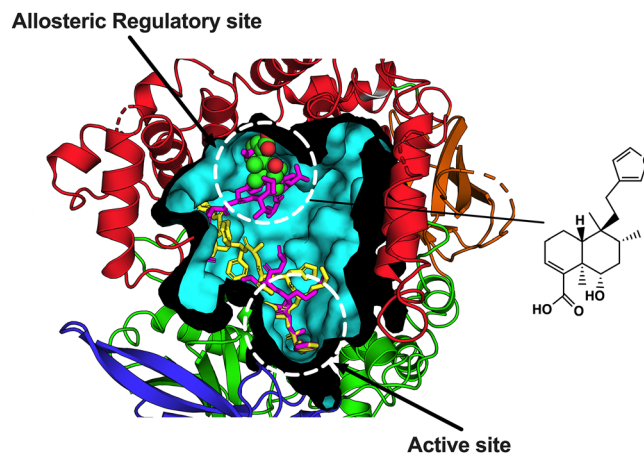

Figure 1. Schematic representation of the internal cavity of ERAP1 (in cyan cutaway view) indicating the active site of the enzyme as well as the allosteric regulatory site that is targeted by the natural product (4aR,5S,6R,8S,8aR)-5-(2-(Furan-3-yl)ethyl)-8-hydroxy-5,6,8a-trimethyl-3,4,4a,5,6,7,8,8a-octahydronaphthalene-1-carboxylic acid, shown in sphere representation inside the regulatory site (the chemical formula is shown on the right). Two peptide substrates crystallized with ERAP1 are shown in stick representation (10 mer peptide in yellow and 15 mer in magenta). Notice how the 15 mer peptide overlaps with the natural product inhibitor at the allosteric site, while the 10 mer does not.

of the C-terminal moiety of the peptide with distal locations at the other end of the cavity and at the intersection of domains II and IV of the enzyme are thought to contribute to conformational closing and activation [25]. Recent crystal structures of ERAP1 in complex with nonhydrolysable peptidic substrates revealed that the *C*-terminus of the peptide can be recognized by a specific allosteric site that features a carboxypeptidase-like motif [26]. Occupation of this site by small peptides or organic compounds can lead to enzyme activation toward small substrate hydrolysis, suggesting that it has a direct regulatory role on enzyme activity. The interplay between the active and this allosteric site has been proposed to underlie at least some of the length selection properties of ERAP1 [26]. Recently, we described a small-molecule inhibitor of ERAP1 that occupies this site and acts as an activator for small substrates but inhibits larger peptidic substrates likely by direct competition with their *C*-terminus [18]. However, crystal structures of ERAP1 with a 15- and 10-mer substrate analogues revealed that, of the two, only the 15-mer peptide *C*-terminus utilized this site and, thus, had direct competition with this allosteric inhibitor [26] (Fig. 1). This finding suggested that not all ERAP1 peptide substrates utilize this allosteric site, and therefore, not all substrates may be affected equally by an allosteric inhibitor targeting this site.

To address the relative importance of the allosteric or regulatory site on the substrate selection of ERAP1 and to understand its role in antigen presentation, we utilized an allosteric inhibitor targeting this site to analyze the effects on the immunopeptidome of a widely used cancer cell line (A375 cell line derived from human skin melanoma, the American Type Culture Collection [ATCC] number CRL-1619) and compare them to the immunopeptidome of WT and *ERAP1* KO cells. Comparison of the inhibitor-treated
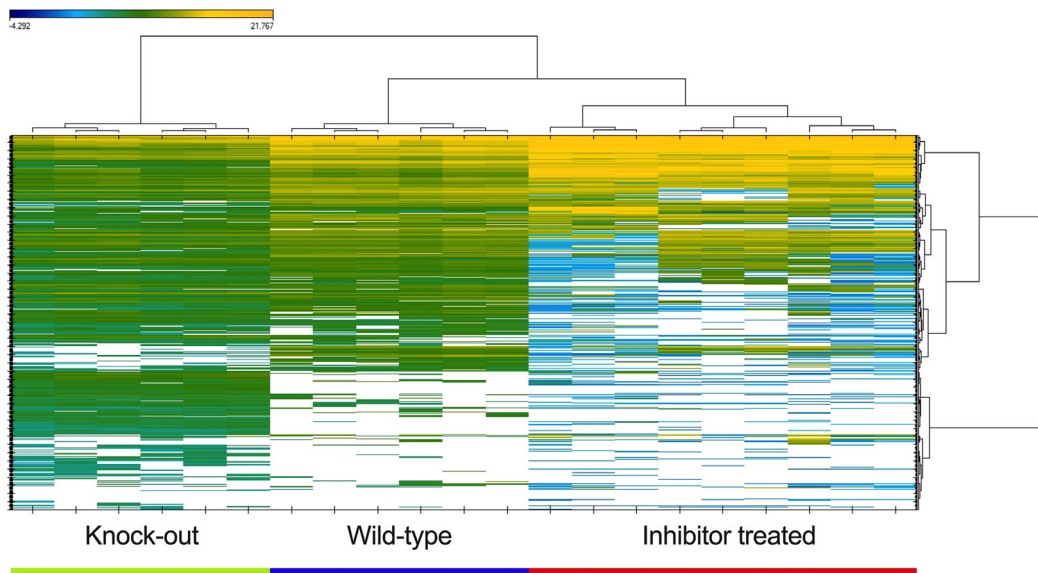
Figure 2. Heatmap and cluster analysis of the detected peptides for each of the experimental conditions (indicated at the bottom). Hierarchical clustering was conducted on 3134 peptides using Manhattan Distance. The peptide intensities are color-coded from blue (low) to yellow (high).

cells to the ERAP1 KO cells allowed us to draw conclusions about the relative importance of this allosteric site on antigenic peptide trimming and presentation in a cellular context. We find that although this site is equally important for immunopeptidome generation, it is not functionally equivalent to the active site. Our findings contribute to our understanding of the complex landscape of ERAP1-mediated antigenic peptide selection and suggest that different modes of inhibition can result in different flavors of immunopeptidome modulation—a critical parameter for the rational development of therapeutic applications.

Results

Analysis of the immunopeptidome of A375 cells

To investigate the functional role of the allosteric regulatory site of ERAP1, we set forth to analyze the effect of targeting that site using an allosteric inhibitor on the immunopeptidome of cells. As a cellular model, we utilized the A375 melanoma cancer cell line since, as previously demonstrated, its immunopeptidome is sensitive to ERAP1 inhibition [5]. In addition, A375 cells express 10–20 fold less amount of ERAP2, thus, minimizing possible compensatory functions from this enzyme [5]. We treated A375 cells with 10 μM of the compound *(4aR,5S,6R,8S,8aR)-5-(2-(Furan-3-yl)ethyl)-8-hydroxy-5,6,8a-trimethyl-3,4,4a,5,6,7,8,8a-octahydronaphthalene-1-carboxylic acid* (Fig. 1) for a total period of 6 days. The utilized concentration is 10-fold higher than the previously measured cellular EC$_{50}$ of this compound and should result in more than 90% inhibition of ERAP1 in the cell [18]. The inhibitor had no observable negative effects on cell viability for concentrations up to 30 μM (Supporting Information Fig. S1). As a positive control, we subjected the same cell line

to CRISRP/Cas9 with a guide RNA targeting the *ERAP1* gene. This led to undetectable ERAP1 expression as evidenced by western blotting and, thus, corresponds to a positive control condition simulating complete inhibition of the enzyme (Supporting Information Fig. S2). WT cells were also analyzed as a negative control. For both WT and KO cells, the inhibitor did not affect MHC-I surface presentation as judged by FACS analysis (Supporting Information Fig. S3). For each condition, we grew the cells to about 0.4–0.5 × 10^9 cells in three separate biological replicates (a total of about 1–1.5 × 10^9 cells per condition). Each condition was later analyzed in triplicate by LC/MS-MS, resulting in a maximum of nine replicates (three biological and three technical) per condition. MHC-I-peptide complexes were isolated by affinity chromatography using the W6/32 antibody as previously described [5]. Eluted peptides from MHC-I complexes were sequenced by LC-MS/MS using data-independent acquisition [27]. One biological replicate for the WT and KO conditions gave a very low peptide signal and was not analyzed further. In total, we identified 3443 unique peptide sequences. A total of 309 peptide sequences were common with a blank injection control and were removed, leaving 3134 unique peptides (Supporting Information Table S1). A heatmap of identified peptides clustered by signal intensity is shown in Fig. 2. All replicates from each experimental condition cluster together validating the reproducibility of the analysis. Visual inspection of the heatmap suggests that there are significant differences between the three conditions, indicating that both pharmacological and genetic inhibition of ERAP1 is sufficient to shift the immunopeptidome, as shown previously [28–30]. Surprisingly, however, the overall profiles of the KO and inhibitor-treated cells were strikingly different, suggesting that the immunopeptidome shifts induced by a total lack of the ERAP1 enzyme or allosteric inhibition are not equivalent.
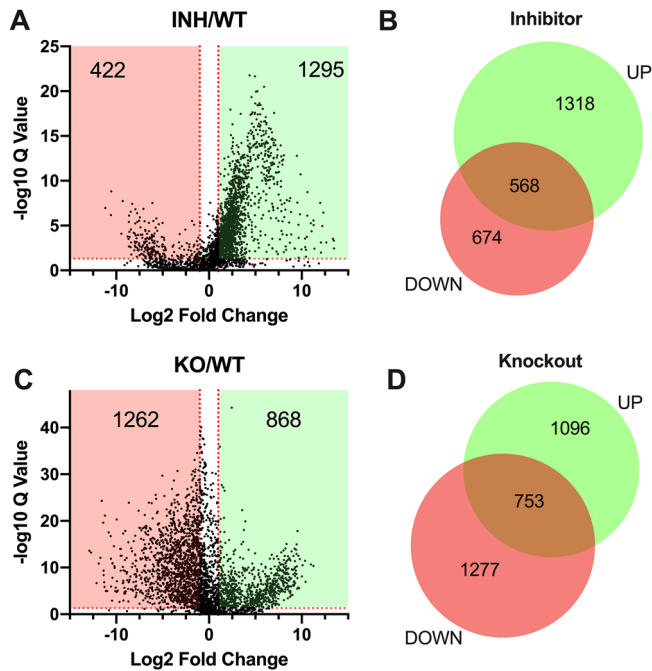
Figure 3. Comparison of identified peptides after pharmacological inhibition (*Panels A-B*) or genetic down-regulation (*Panels C-D*) of ERAP1 compared to WT cells. *Panels A and C*, volcano plots comparing two conditions at a time (inhibitor versus WT and KO versus WT) indicating the correlation between relative abundance change and statistical significance. Each dot represents a separate peptide. Colored boxes (red and green) contain peptides that show a significant (over twofold) change between conditions and statistical significance (Q value < 0.05). *Panels B and D*, Venn diagrams depicting the overlap between peptides upregulated or downregulated by either the inhibitor or the KO, including unique peptides not depicted in panels A and C.

Figure 4. Principal component analysis of the three experimental conditions. Each point represents a separate experiment that belongs to the indicated experimental condition. All experiments of each condition cluster together as indicated by the colored circles.

Chemical inhibition or genetic down regulation induces major immunopeptidome shifts

To better understand the differences in peptide presentation between the three conditions, we performed a pairwise analysis of the conditions that disrupt ERAP1 function (inhibitor or KO) and the WT cells. The volcano-type plots for these comparisons are shown in Fig. 3. Comparing the inhibitor-treated cells to the WT, 1295 peptides were upregulated by more than twofold and in a statistically significant manner (Q value $\geq$ 0.05) (Fig. 3A). Similarly, 422 peptides were downregulated. In addition, 23 peptides were found in the inhibitor-treated cells but not identified in the WT cells, and 252 peptides were unique to the WT cells and were not present in the inhibitor-treated cells. By summing the quantitatively affected with the unique peptides, we concluded that the presentation of 1318 peptides was enhanced by the inhibitor and 674 peptides were downregulated (Fig. 3B). A similar analysis of the comparison of the effect of the KO indicated that from 3125 peptides detected, 1095 peptides were upregulated by the KO, and 1277 peptides were downregulated (Fig. 3C and D). Overall, the inhibitor resulted in the upregulation of 51% and the downregulation of 26% of the immunopeptidome of A375 melanoma cells and the KO resulted in the upregulation of 35% and the downreg-

ulation of 41% of the immunopeptidome. In summary, although the effect of ERAP1 modulation was relatively small in terms of novel sequences presented, it was major in terms of changes in the levels of presentation of existing peptides.
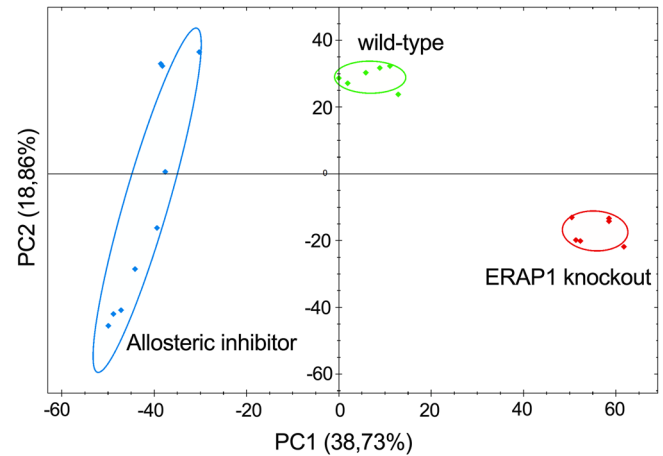
Principle component analysis

While both ways to interfere with ERAP1 function yielded similar, albeit not identical, overall effects on the immunopeptidome, the exact nature of the peptides presented was different. To compare the different experimental conditions, we performed principal component analysis (Fig. 4). This analysis indicated that, while all experiments from each condition clustered together, all three conditions were distinct, suggesting statistically significant changes in the sequence patterns of peptides generated.

Analysis of peptide length

Since length is a key parameter for MHC-I binding, we analyzed the length distribution of peptides identified to be either upregulated or downregulated in each condition. ERAP1 has been shown to both help generate correct-length peptides for MHC-I and to also over-trim peptides to lengths too short for binding. Peptides in the WT cells that were unaffected by ERAP1 disruption were primarily 9 mers as expected based on the binding preferences on MHC-I (Fig. 5). The inhibitor-downregulated and KO-downregulated peptides showed a similar distribution. The KO-upregulated peptides were primarily 10 and 11 mers consistent with a lack of a length-limiting aminopeptidase. Strikingly, although the inhibitor-upregulated peptides also displayed a shift toward longer peptides, this effect was much less pronounced compared to the KO-upregulated peptides, with most peptides being 9 mers. Statistical evaluation of the length distribution for
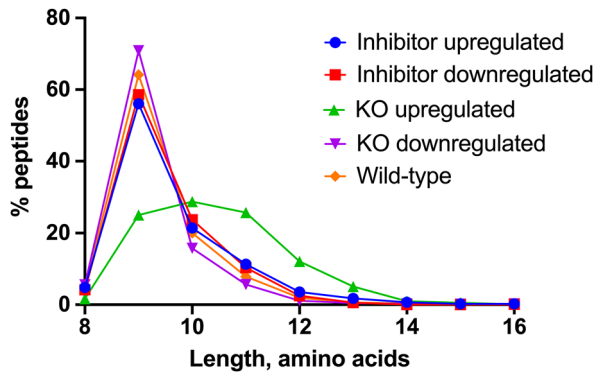
Figure 5. Distribution of lengths of detected peptides for each experimental condition (inhibitor treatment, ERAP1 KO or WT) and abundance change (upregulated or downregulated peptides).

each experimental condition using the ggbarstats() plot from the ggstatsplot R Package [31] confirmed the statistical significance of the changes in peptide length distribution in the KO compared to the WT, whereas no statistical significance was found when comparing the effects of the inhibitor to the WT (Supporting Information Fig. S4 and S5). This surprising result suggests that ERAP1 inhibition through the allosteric regulatory site does not sufficiently reduce the processing of longer peptides to allow their accumulation as it occurs in the complete absence of the enzyme.

Peptide affinity for MHC-I alleles

To validate that the identified peptides are indeed ligands of the MHC-I haplotypes carried by A375 cells (HLA-A*01:01:01, HLA-A*02:01:01, HLA-B*44:03:01, HLA-B*57:01:01, HLA-C*06:02:01, and HLA-C*16:01:01), we used the HLAthena server to score the peptides with lengths between 8 and 11 amino acids for predicted binding to at least one HLA allele [32]. In all experimental conditions, over 90% of identified peptides scored a rank below 2 and are, thus, considered binders for at least one of the MHC-I alleles carried by A375 cells (Fig. 6). In comparison, more than 95% of a randomly generated set of peptides are predicted not to bind to any of the MHC-I alleles. This finding provides validation that the peptides identified are indeed eluted from MHC-I but also suggests that there is no significant change in peptide affinity between peptides affected by the inhibitor or the ERAP1 KO. Thus, both pharmacological and genetic inhibition of ERAP1 can affect the immunopeptidome in qualitative and quantitative manners without degrading the binding capacity of the presented peptides. This finding is in contrast with initial observations that ERAP1 functional disruption leads to the presentation of suboptimal peptides [33].

Presentation of known antigenic peptides

To investigate whether the different modes of ERAP1 perturbation could translate to different cellular antigenicity, we searched iden-
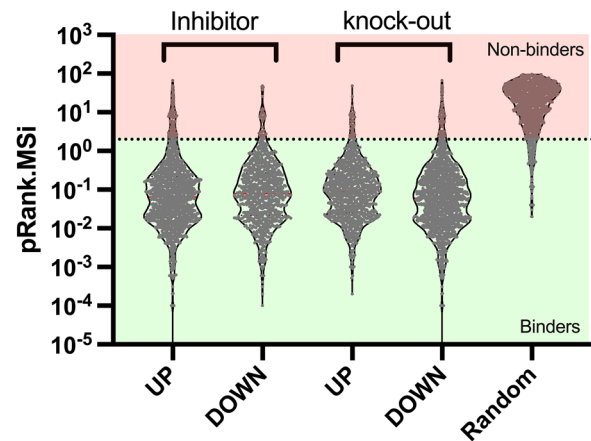

Figure 6. Distribution of the predicted affinities (by HLAthena [32]) of the peptides for the HLA alleles that are expressed by A375 cells (HLA-A*01:01:01, HLA-A*02:01:01, HLA-B*44:03:01, HLA-B*57:01:01, HLA-C*06:02:01 and HLA-C*16:01:01). Each point represents a unique peptide sequence. For each peptide only the score for the best predicted HLA-allele is plotted. A set of peptide sequences generated from a random protein sequence by RandSeq (https://web.expasy.org/randseq/) were also plotted as a negative control. Prediction scores below 2 (dotted line) signify binders to at least one of the tested HLA alleles.

tified peptides for known melanoma cancer antigenic peptides from the MAGE-A tumor-associated antigen and the P-antigen family [34]. Table 1 lists identified peptides. The inhibitor-treated cells demonstrated a distinct pattern compared to the KO cells and upregulated the presentation of most MAGE-A antigenic peptides. This finding suggests that allosteric inhibitors may indeed be useful in enhancing the antigenicity of cancer cells.

Comparison of two modes of ERAP1 functional disruption

For a more direct comparison of the immunopeptidomes of the inhibitor-treated and KO cells, we performed a volcano-type analysis, shown in Fig. 7A. From this analysis, it was evident that many peptides are differentially regulated by the inhibitor compared to the KO cells. Accordingly, 516 peptides were upregulated in the KO compared to the inhibitor, and 1487 were downregulated. Most importantly, when comparing the lists of upregulated or downregulated peptides by the inhibitor or the KO compared to the WT cells (data presented in Fig. 3), up to two out of three of the peptides were distinct (Fig. 7B). Thus, it appears that although both the inhibitor and the KO induce significant shifts in the immunopeptidome of A375 cells, these shifts have a very limited overlap, a finding that suggests significant mechanistic differences between the two methods of ERAP1 disruption.

Presentation by different HLA alleles

The observed differences in peptides presented when ERAP1 is disrupted by different methods may be translated to the cell

Table 1. List of cancer antigenic peptides that are affected by the inhibitor or the KO

Antigenic peptide	Gene	Inhibitor upregulated	Inhibitor downregulated	Knock-out upregulated	Knock-out downregulated
MEVDPIGHLY	MAGEA3		+		+
KEADPTGHSY	MAGEA1	+		+	
EVDPIGHLY	MAGEA3	+			+
GVYDGREHTV	MAGEA4	+			
KVLEHVVRV	MAGEA4	+			
FVYGEPREL	MAGEC2	+			+
EEVPSGVIPNL	MAGEC2	+			
EVDPTSHSY	MAGEA11	+			
YGEPRKL	MAGEA9	+			
TLPTFDPTKV	PAGE5				+
SAYGEPRKL	MAGEA1		+	+	

surface presence of different HLA alleles. To address this question, we calculated the relative percentage of peptides predicted to bind best to one of the six HLA alleles carried by A375 cells (Fig. 8). Interestingly, when comparing the inhibitor to the KO, the inhibitor-treated cells presented more peptides bound onto HLA-A*01:01, whereas the KO cells presented more peptides, onto HLA-B alleles. The overall pattern was largely reversed for the downregulated peptides, in which the inhibitor showed enhancement for HLA-B alleles. Thus, it appears that the different modes of ERAP1 functional disruption can be reflected in the relative presentation of HLA alleles.
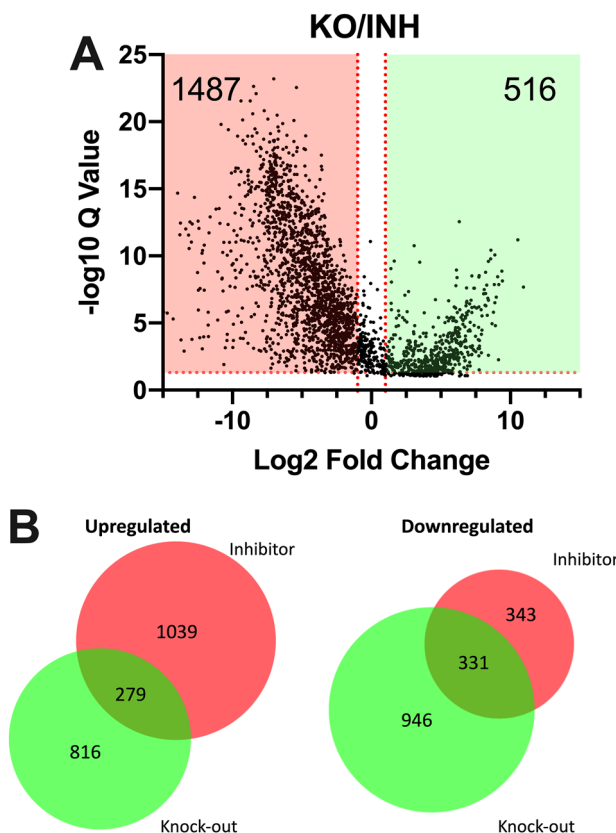
Analysis of peptide motifs

The observation that the two different modes of inhibition may translate to changes in the presentation by specific HLA alleles, suggested that changes in the sequence motifs of presented peptides may be observable. Although ERAP1 activity has been reported to be sequence-dependent, how well ERAP1 sequence specificity translates to surface presentation is not well understood [14, 26, 35]. While ERAP1 can edit the peptide repertoire in the ER, HLA binding specificity, and editing chaperones, such as the peptide loading complex, may filter out most of the ERAP1 sequence selectivity [7]. To approach this question, we performed nonmetric multidimensional scaling (NMDS) [36]. This analysis projects peptides in two-dimensional space based on the similarity of the AA sequences. We performed pairwise comparisons of the inhibitor upregulated versus the KO upregulated peptides predicted to bind to at least one HLA allele (as in Fig. 6) as well as the inhibitor downregulated versus the KO downregulated binders (Fig. 9). For the upregulated peptides, the stark difference in length distribution between the inhibitor-treated cells and the KO cells (Fig. 5), would bias the analysis toward the most populated clusters and, thus, we focused our analysis on the 10 mers, which are roughly equal in numbers in both conditions. NMDS analysis revealed five major clusters (Fig. 9A) and distinct patterns for co-clustered peptides, with inhibitor-upregulated peptides positioned in a different way than KO-upregulated peptides (Fig. 9B). In an attempt to quantify the differences, the 181 inhibitor-upregulated (Fig. 9C, in red) versus the 224 KO-upregulated (Fig. 9C, in green) peptides were plotted per cluster. Statistical analysis revealed that inhibitor-upregulated peptides were overrepresented in cluster 5 ($\times 2$, Bonferroni n = clusters, p_{adj} = 4.46e-03), while the

Figure 7. Panel A, Volcano plot comparing the inhibitor effect to the knock-out effect. Each point corresponds to a separate peptide sequence. Red points correspond to peptides with an abundance that was different by at least twofold between conditions and are statistically significant. **Panel B,** Venn diagrams summarizing the observed overlap between the peptides upregulated (left) or downregulated (right) compared to the WT cells in either the inhibitor-treated or the KO cells.
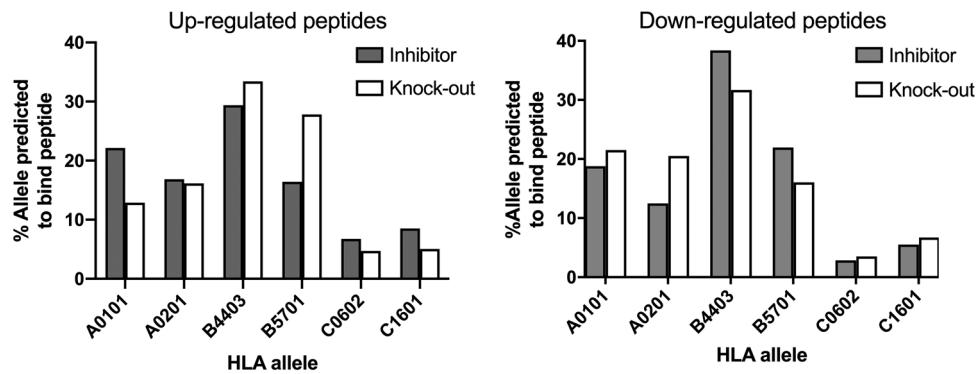
Figure 8. Distribution of HLA-alleles predicted to bind the identified peptides that are upregulated or downregulated by the inhibitor or in the knock-out cells. Predictions were performed with HLAthena as in Fig. 6.

KO-upregulated peptides were overrepresented in clusters 1 ($\times 2$, Bonferroni n = clusters, p_{adj} = 4.07e-05) and 2 ($\times 2$, Bonferroni n = clusters, p_{adj} = 2.1e-04). Cluster 1 (Fig. 9D) fits the sequence motif of HLA-B*57:01, cluster 2 the motif of HLA-B*44:03 and HLA-A*02:01, whereas cluster 5 is typical for HLA-A*01:01. These results are in concordance with the results shown in Fig. 8, which indicate a shift from HLA-A*01:01 in the inhibitor-treated cells to HLA-B*57:01 in the KO cells. Cluster 5 differs from the other two clusters mainly in position 3, where D is the most abundant AA, and position 10, which is occupied only by Y. These positions are also anchor positions for the represented allele. Cluster 1 is characterized by S, T, A, & V in position 2 and W and F in position 10, which are also considered anchor positions for HLA-B*57:01. Furthermore, position 1 is dominated by the positively charged amino acids K and R, which are considered poor substrates for ERAP1 [37]. These amino acids are not unusual for this allele, as seen in Supporting Information Fig. S2, and could indicate that peptides that do not require ERAP1 for trimming, which are expected to be represented to a higher extent upon complete inhibition of the enzyme, are preferred in this case.

For the downregulated peptides NMDS analysis, we again focused our analysis on the 10 mers, which are roughly equal in numbers between the two conditions (Fig. 9E-H). Cluster 3 was significantly overrepresented in KO-downregulated peptides ($\times 2$, Bonferroni n = clusters, p_{adj} = 0.022). A similar trend was seen for cluster 6, which, however, was not statistically significant after multiple comparison corrections ($\times 2$, Bonferroni n = clusters, p_{adj} = 0.087, p = 0.012). Cluster 2 was overrepresented by inhibitor-downregulated peptides, although with low statistical significance ($\times 2$, Bonferroni n = clusters, p_{adj} = 0.066, p = 0.009). Sequence motifs in clusters 2 and 3 (Fig. 9D) are representative of HLA-B*44:03. Although this allele was the most presented in the upregulated peptides of both treated samples, some differences in the exact preferences would still be possible, and it may as well be that depending on the treatment (inhibitor or KO), different submotifs may be affected. The motif depicted in cluster 6, which includes the most KO-downregulated peptides (30% of KO-downregulated 10 mers) matches the preferences of HLA-A*01:01 and, despite poor statistical significance,

further supports the observation that the presentation of peptides to this allele is negatively affected. Finally, cluster 5, was more populated in the KO and fits HLA-A*02:01 consistent with the results in Fig. 6. Overall, NMDS analysis suggested that while presented peptide sequences are dominated by HLA binding preferences, different methods of perturbation of ERAP1 function can still influence the relative abundance of HLA-compatible sequence motifs. How exactly ERAP1 substrate preferences and the ERAP1 allosteric site can regulate the ER repertoire of "MHC-ready" peptides will likely require integrated analysis in more controlled systems to help deconvolute the relative influence of these antigen processing components.

Discussion

Chemical inhibition of ERAP1 is currently an emerging therapeutic direction for both cancer immunotherapy and HLA-associated autoimmunity [16, 45]. The main mechanistic premise for those approaches is the regulation of the immunopeptidome, allowing the manipulation of the peptide repertoire that T cells explore on the cell surface and, as a result, the modulation of T-cell activation. This could be useful in cancer immunotherapy by either the upregulation of existing or presentation of novel cancer neoantigens [46], which would enhance existing or generate novel immune responses against the tumor. Conversely, in the case of HLA-associated autoimmunity [47], the downregulation of specific self-peptides that activate disease-associated cytotoxic T cells could have therapeutic applications [48, 49]. In both cases, the therapeutic outcome could result from manipulating the presentation of a few antigenic peptides, which can be achieved by inducing "surgical" shifts to the immunopeptidome of the cells. Inhibition of ERAP1 has been shown to be a promising avenue toward this, although much is still unknown about the exact regulatory pressure that ERAP1 can induce on the immunopeptidome. Indeed, although ERAP1 has been reported to be absolutely necessary for the generation and the destruction of specific antigenic epitopes [9, 50], its overall effect on the immunopeptidome varies between major and limited, depending on the system studied [33,
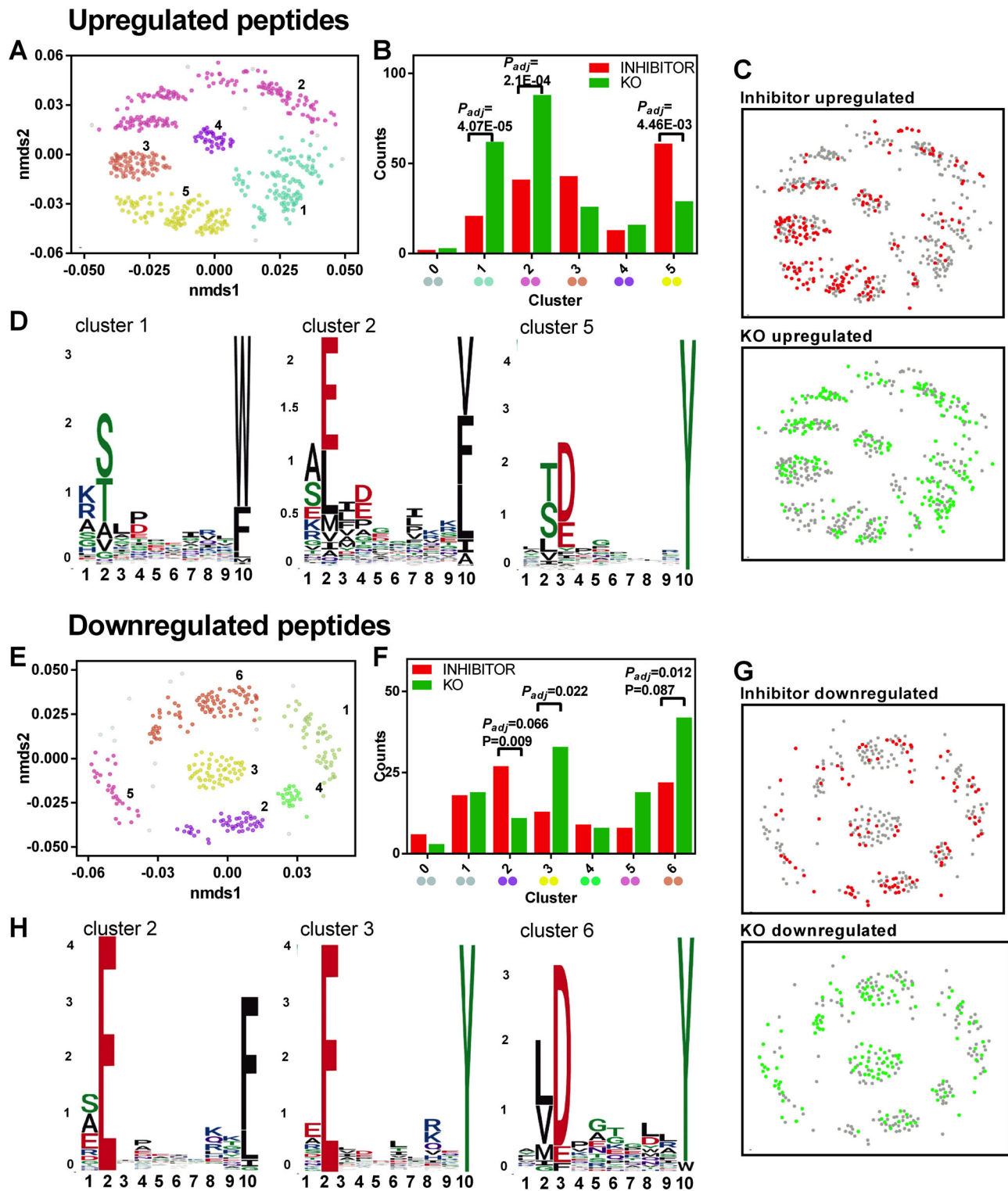
Figure 9. Nonmetric multidimensional scaling analysis of the peptide sequences that are affected by inhibitor treatment versus the ERAP1 KO. Panels A-D, comparison of the upregulated peptides and Panels E-H, comparison of the downregulated peptides. Panels A, C, E, and G show two-dimensional representations of discovered clusters each indicated with a different color. Panels B and F show the distribution of the number of peptides for each sequence cluster. *p*-Values are indicated only for statistically significant differences. Panels D and H show the motifs for peptides that are regulated in a statistically significant manner between the two methods of ERAP1 perturbation.

51]. Thus, more detailed knowledge of the effects of ERAP1 on the presented peptide repertoire is necessary to design effective therapeutic interventions.

Although ERAP1 inhibitors targeting the active site have been developed [17], recurring limitations with selectivity versus other aminopeptidases in the family due to the conservation of active site pharmacophores have raised concerns about their clinical usefulness. As an alternative, allosteric inhibitors are being explored [18–20]. Due to thier mechanistic relevance, compounds are of particular interest that target a regulatory site in ERAP1 that accommodates the *C*-terminus of some peptides and helps self-activate their trimming [26]. Potential mechanisms of inhibition for allosteric inhibitors of ERAP1 have been proposed, including direct competition with the *C*-terminus of the peptide or the induction of conformational changes that lock the enzyme in an inactive conformation [18, 25]. However, although allosteric inhibitors appear to have superior selectivity, their effect on the immunopeptidome of cells has not been explored, despite being a critical parameter for translational efforts.

In this study, we compared two methods of disruption of ERAP1 activity on the immunopeptidome of a cancer cell line: genetic KO and allosteric inhibition. Although the most simplistic result would be that the two methods are equivalent, this is not what we find. Both methods of ERAP1 functional disruption do generate substantial shifts on the immunopeptidome, and identified peptides are good MHC-I ligands and carry sequence motifs consistent with the HLA alleles carried by the cells. However, the two methods differ in both their effects on peptide length and specific sequences presented. While the KO leads to the presentation of longer-length peptides (mostly 10 and 11 mers), consistent with previous findings using active-site inhibitors or ERAP1 variants of varying activities [5, 28, 30], the inhibitor had only a marginal effect on length. Despite the limited effect on length, inhibitor treatment led to a shift in presented sequences that is comparable to that of the KO cells and led to the upregulation of the presentation of known melanoma epitopes. This lack of significant effect on peptide length may signify the mechanistic nuances of allosteric inhibition; indeed, in a recent crystal structure of ERAP1 with a 10mer substrate analogue, the *C*-terminus of this peptide was not found to interact with the regulatory site but rather utilize an alternative site in the interface of domains II and IV [26]. If this structural motif is common to other 10 mer peptides, this could explain the lack of accumulation of 10 mers when ERAP1 is inhibited by the regulatory site. This finding suggests that the choice of inhibitory mechanism for ERAP1 could be a powerful tool for manipulating the length of presented peptides in cells.

Several mechanisms could contribute to the stark differences in the presented peptides between the two methods of ERAP1 functional disruption: (A) Less than full inhibition of ERAP1 activity by the inhibitor could allow the trimming of peptides that are especially sensitive to ERAP1. Indeed, based on known cell IC50 values for the compound used [18], the concentration used in these experiments should reach over 90% target engagement, and achieving 100% inhibition with a compound is not always realis-

tic in a pharmacological setting. Still, a previous study using an active-site ERAP1 inhibitor [17], showed effects on peptide length although the target was unlikely to be saturated, suggesting that the lack of 100% engagement is not responsible for the observed effects here, although it could be a contributing factor. In addition, if limited inhibition is the only mechanism, then the inhibitor-treated cells should present a subset of peptides compared to the KO with a higher expected overlap. (B) The KO cells completely lack ERAP1 and this may affect cellular functions by additional mechanisms apart from ERAP1 trimming activity. For example, ERAP1 has been reported to make protein–protein interactions with ERp44 and ERAP2 [52–54], and thus, lack of ERAP1 could induce compensating proteome changes in the cells that could indirectly influence the immunopeptidome. In addition, ERAP1 can be secreted by cells and have functional roles irrespective of its enzymatic activity, which would only be disrupted in the KO cells [55]. (C) Unaccounted-for, off-target effects by either the inhibitor or the KO could also contribute to the differences. D) As stated above, the specific functionality of the allosteric regulatory site could underlie the effects observed in this study. Some evidence already exists that supports this hypothesis [26] and would suggest that some allosteric inhibitors may be substrate-specific and not universal. This, however, has not been explicitly demonstrated yet.

Interpretation of the results of this study should be performed in the context of some important limitations of our experimental setup. These would include partial target engagement by the inhibitor and possible off-target effects by either the inhibitor or the KO. In addition, the low background expression of ERAP2 could partially compensate for the lack of ERAP1 activity and reduce observed effects, at least for some epitopes, as recently reported [56]. Furthermore, we have not addressed whether other chemical scaffolds that target the regulatory site have the same effects [20]. In addition, little is known about how the inhibitor affects the kinetics of antigen presentation. We chose to incubate the cells for 6 days over three passages to best simulate a therapeutic setting with cancer cells growing in the presence of a drug, but this is not necessarily identical to the steady-state changes brought over by the genetic KO. Given our results, further studies using in cellulo site-directed mutagenesis in the active and allosteric sites may be necessary to clearly deconvolute the role of the allosteric site under steady-state conditions.

Regardless of possible limitations, our findings can have important consequences for translational efforts focusing on manipulating ERAP1 activity to modulate the immunopeptidome. Currently, ERAP1 is being explored as a target for therapeutic interventions in both cancer immunotherapy and HLA-associated autoimmunity, and those efforts revolve around immunopeptidome modulation [15, 16, 21]. While both active-site and allosteric inhibitors are being explored, the superior selectivity of allosteric inhibitors may make them preferred for clinical development. Our results suggest that targeting the allosteric regulatory site affords unique opportunities in modulating the immunopeptidome that are nevertheless distinct from a KO

control or possibly an active-site inhibitor. As a result, if the therapeutic outcome of ERAP1 functional disruption hinges on the presentation, or lack thereof, of a particular peptide epitope, different methods of inhibition need to be evaluated on a case-by-case basis. In addition, the KO control that is often used in evaluating the efficacy of inhibitors needs to be carefully evaluated for how well it can be translated to a therapeutic setting.

In summary, we evaluated the relative effect of an allosteric inhibitor on the immunopeptidome of a cancer cell line and discovered a series of unexpected major effects compared to the KO control that likely stem from poorly understood mechanistic nuances of the regulatory allosteric site. Our results highlight ERAP1 as a flexible target for modulating the immunopeptidome of cells but also instigate caution for carefully engineering immunopeptidome shifts for therapeutic applications.

Materials and methods

Cell lines

The A375 human malignant melanoma cell line and the W6/32 hybridoma cell line (CRL-1619 and HB-95, respectively) were purchased from ATCC and used as provided by the vendor.

Generation of a KO A375 cell line

To generate ERAP1 KO A375 cells, the pSpCas9(BB)-2A-Puro (PX459) V2.0 vector was used. The PX459 vector was a gift from Feng Zhang (Addgene plasmid # 62988; http://n2t.net/addgene:62988; RRID: Addgene_62988). To disrupt the *ERAP1* gene, the regions: 5'- ggttgcaagggaccatttga-3' in the antisense clone and 5'-gctatcggaagaacccctgc-3' in the sense clone of ERAP1 exon 2 were targeted. The two DNA oligo sets (Guide 1: 5'-caccggttgcaa-gggaccatttga-3', Guide rc 1: 5'-aaactcaaatggtcccttgcaacc-3' and Guide 2: 5'-caccgctatcggaagaacccctgc-3', Guide rc 2: 5'-aaacgcaggggttcttccgatagc-3') were phosphorylated by T4 polynucleotide kinase (New England Biolabs cat. no. #M0201) by incubating for 30 min at 37°C and then allowed to anneal after incubating for 5 min at 95°C. The oligos were cloned into the pX459 vector using the fast digest BbsI restriction enzyme (New England Biolabs cat. no. #R0539) as previously described [38]. A375 cells were transfected with the plasmids at a 1:1 ratio, using Lipofectamine 2000 (Thermo Fisher Scientific) following the manufacturer's instructions. Twenty-four hours after transfection, A375 cells were treated with 1.5 mg/mL of puromycin (Applichem) for 48 h. Single-cell clones were isolated by limiting dilution. Out of 18 A375 clones that were isolated, five (#3, #5, #9, #10 and #13) did not express ERAP1. ERAP1 expression was checked with Western blot analysis.

Western blotting

About 5×10^5 A375 cells were lysed through three cycles of freeze thaw in PBS buffer containing 500 μM PMSF. Cell lysates were centrifuged at 12 000 rpm at 4°C for 30 min and the supernatant was carefully collected. Whole cell lysates were analyzed with SDS–PAGE under reducing conditions in a 10% polyacrylamide gel. The separated proteins were blotted onto a polyvinylidene difluoride membrane (Thermo Scientific, 88520) using the antibody of human aminopeptidase PILS/ARTS1 polyclonal goat IgG (R&D Systems, AF2334) for ERAP1. Primary antibody was used at a final concentration of 2 μg/mL and the secondary antibody, anti-goat IgG-HRP (HAF017) purchased from R&D Systems, was diluted 1:1000. As an HRP substrate, we used Pierce chemiluminescent western blotting substrate (Thermo Scientific, 32209) and enhanced chemiluminescence was detected in LAS 4000 (Fujifilm). The images were processed using the AIDA Image analysis software (Elysia-Raytest).

Treatment of A375 cells with inhibitors

A375 cells were treated with 10 μM of the compound (4aR,5S,6R,8S,8aR)-5-(2-(Furan-3-yl)ethyl)-8-hydroxy-5,6,8a-trimethyl-3,4,4a,5,6,7,8,8a-octahydronaphthalene-1-carboxylic acid [18] for 6 days over three passages, with the inhibitor being refreshed every 2 days. After 6 days, cells were detached using Accutase™ (Thermo) and harvested by centrifugation. Cell pellets were stored in −80°C until needed for analysis.

Cytotoxicity assay

A375 cells (2500 cells/well) were cultured in the presence of 0–100 μM of compound for 48 h. The culture medium was replaced by 100 μL of DMEM containing 1 mg/mL MTT reagent (3-(4,5-dimethylthiazol-2-yl)-2,5-diphenyl tetrazolium bromide, Merck, MA, USA) and incubated for another 4 h. The resultant formazan crystals were dissolved in 100 μL of DMSO and the absorbance intensity was measured on a TECAN infinite M200 microplate fluorescence reader at 540 nm with a reference at 620 nm. All experiments were performed in duplicate.

Flow cytometry

One million cells per sample were transferred to FACS tubes and washed twice with 1 mL FACS buffer (1%BSA/PBS, 0.02% NaN₃). The cells were stained with 2 μL undiluted W6/32-FITC (Bio-Rad, MCA81F) for 30 min on ice. After incubation, the cells were washed with 2 mL FACS buffer, centrifuged at 4°C at 200*g* for 5 min, and resuspended in 300 μL FACS buffer. The samples were analyzed in a FACScalibur flow cytometer using the BD CellQuest™ Pro software. Approximately 20 000 events per sample were measured.

Preparation of immunoaffinity columns

The preparation of the immunoaffinity columns with the W6/32 antibody has been previously described [5, 39]. The W6/32 antibody was purified from the supernatant of the hybridoma cell line HB-95™ (ATCC) by affinity chromatography using protein G agarose beads. The purified antibody was dialyzed in coupling buffer (NaHCO$_3$ 0.1 M, NaCl 0.5 M, pH 8.3) overnight. A total of 0.285 g of dry beads of cyanogen bromide-activated Sepharose 4B (GE Healthcare 17-0430-01) were used per column. Also, a total of 2 mg of purified antibody was added to the beads and left for coupling overnight at 4°C, and then washed with coupling, then with blocking buffer (Tris-HCl 0.1 M, pH 8.0), and then incubated with blocking buffer for 3 h at room temperature. Finally, columns were washed with acidic (CH$_3$COONa 0.1 M, NaCl 0.5 M, pH 4.0) and basic (Tris-HCl 0.1 M, NaCl 0.5 M, pH 8.0) buffer and equilibrated with 20 mM Tris-HCl, pH 7.5, 150 mM NaCl. Precolumns were also constructed with the same method except for the W6/32 coupling step.

Isolation of peptides bound onto MHC-I from cells

For the isolation of MHC-I from cells, the procedure was followed as described [5]. Briefly, about 5×10^8 cells were used per biological replicate. Cells were lysed with 20 mL buffer containing Tris-HCl, pH 7.5, 150 mM NaCl, 0.5% IGEPAL CA-630, 0.25% sodium deoxycholate, 1 mM EDTA, pH 8.0, and one complete EDTA-free protease inhibitor cocktail tablet for 1 h at 4°C. The cell lysate was cleared with ultracentrifugation at 1 00 000 g and then loaded onto a W6/32 affinity column. The column was washed using 20 mM Tris-HCl, pH 8.0, 150 mM NaCl, and then using 20 mM Tris-HCl, pH 8.0, 400 mM NaCl. Elution of the MHC-I and bound peptides was achieved by 1% TFA. The peptides were further purified from the MHC-I using reversed-phase C18 disposable spin columns (Thermo Scientific).

LC–MS/MS analysis

The peptidic samples were cleaned up by a SP3 strategy [40] using a 1:1 Sera-Mag Carboxylate SpeedBeads mixture (Sigma-Aldrich, Cat. #45152105050250 and Cat. #65152105050250). In short, the beads and the peptides were incubated for 30 min in an 98% acetonitrile solution. The peptides on beads were subjected to two washing steps with 100% acetonitrile and finally eluted from the paramagnetic beads using water with 0.1% formic acid.

Equal amounts of peptide mixtures were analyzed by LC–MS/MS in three technical replicates. LC–MS/MS analysis was performed by injecting the peptidic eluate directly onto an analytical column (75 μm I.D. × 25 cm, C18, pepsep), followed by gradient elution (Ultimate3000 RSLC system; 7–45% B in 18 minutes; A = 0.1 % formic acid in water, B = 0.1% formic acid in acetonitrile) with a flowrate of 400 nL/min. The separated peptides were ionized and sprayed into the mass spectrometer (Q Exactive™ HF-X mass spectrometer, Thermo, Waltham, MA) through a pepsep sprayer equipped with a liquid junction stainless steel emitter. The spectrometer was operated in data-independent mode, in the scan range of 375–1100 m/z using 120 K resolving power with an automated gain control (AGC) of 3×10^6 and max IT of 60 ms, followed by data-independent analysis using 8 Th windows (39 loop counts) with 15 K resolving power with an AGC of 3×10^5 and max IT of 22 ms and a normalized collision energy of 26.

Data analysis

Orbitrap raw data were analyzed in DirectDIA mode using the Spectronaut™ software version 16 (Biognosys) [27] through searching against the reviewed Human Uniprot database (retrieved 4/21, 49,852 entries) in the library-free mode of the software, in an unspecific digest search mode with a peptide size range of 7 to 20 amino acids. Hierarchical clustering was performed using Manhattan Distance.

Nonmetric multidimensional scaling analysis

For the NMDS analysis, we considered two comparisons separately: inhibitor versus KO-upregulated binders and inhibitor versus KO-downregulated binders. The results from Spectronaut®'s unpaired t-test were used as input, after filtering for binding affinity using HLAthena. Significantly upregulated binders (q- value ≤ 0.05, log$_2$diff ≥ 1, HLAthena score ≤ 2) in the inhibitor-treated versus the WT and in the KO versus the WT cells were used for the identification of patterns in the upregulated peptides, while significantly downregulated binders (q-value ≤ 0.05, log$_2$diff $\leq$ -1, HLAthena score ≤ 2) in the inhibitor-treated versus the WT and in the KO versus the WT condition were used as input for the identification of patterns in the downregulated peptides. Next, we performed NMDS of 10-mer peptides using entropy-weighted peptide distances in two-dimensional space according to the method of Sarkizova et al. [32] [(MolecularEntropy() function from HDMD R package], as described in [41], with some modifications. Peptide distances in two dimensions were mapped by using NMDS with 10 separate ordinations of 500 iterations with the nmds() function from the ecodist R package [36]. The configuration with the least stress was used for visualization of the immunopeptidome. Then, we used density-based spatial clustering for applications with noise (DBSCAN) [42] [fpc R package] to cluster peptides according to the elbow method for the estimation of the number of clusters that fit the data [KNNdistplot function() in dbscan R package [43]]. Eps parameter was set to 0.0082 and 0.011 for the comparison of the upregulated and the downregulated peptides, respectively. Differences in the number of affected peptides per cluster were assessed by using a chi-squared test [chisq.test() in rbase] and the derived p-values were adjusted

(*p*adj) using the Bonferroni method. Ggseqlogo *R* package as used to generate sequence logo plots [44].

Conflict of interest: All authors declare no commercial or financial conflict of interest.

Author contributions: IT performed all steps of the immunopeptidome isolation, analyzed proteomic data, cell viability measurements, and interpreted results. MS and GP performed the LC—MS/MS analysis, analyzed data, and helped with interpretation. DK generated and characterized the ERAP1 KO cell line and performed the FACS analysis. MK and JK performed the NMDS analysis and helped analyze data and interpret results. ES conceived and supervised the project, analyzed data, interpreted results with help from all authors, and wrote the first draft of the manuscript. All authors have contributed to the authoring of this manuscript and have agreed to its final version.

Data availability statement: All data described are available in the article and associated supporting information. Numerical values used for the generation of graphs are available upon request to the corresponding author (Efstratios Stratikos; E-mail: estratikos@chem.uoa.gr or stratos@rrp.demokritos.gr). The MS proteomics raw data have been deposited to the ProteomeXchange Consortium via the PRIDE [57] partner repository with the dataset identifier PXD039584 (http://www.ebi.ac.uk/pride/archive/).

Peer review: The peer review history for this article is available at https://publons.com/publon/10.1002/eji.202350449

References

1 **Rock, K. L., Reits, E. and Neefjes, J.,** Present yourself! By MHC class I and MHC class II molecules. *Trends. Immunol.* 2016. **0**: 1–14.

2 **Weimershaus, M., Evnouchidou, I., Saveanu, L. and van Endert, P.,** Peptidases trimming MHC class I ligands. *Curr. Opin. Immunol.* 2013. **25**: 90–96.

3 **Admon, A. and Bassani-Sternberg, M.,** The human immunopeptidome project, a suggestion for yet another postgenome next big thing. *Mol. Cell. Proteomics* 2011. **10**: 1–4.

4 **Atkinson, E. A. and Bleackley, R. C.,** Mechanisms of lysis by cytotoxic T cells. *Crit. Rev. Immunol.* 1995. **15**: 359–384.

5 **Koumantou, D., Barnea, E., Martin-Esteban, A., Maben, Z., Papakyriakou, A., Mpakali, A., Kokkala, P. et al.,** Editing the immunopeptidome of melanoma cells using a potent inhibitor of endoplasmic reticulum aminopeptidase 1 (ERAP1). *Cancer Immunol. Immunother.* 2019. **68**: 1245–1261.

6 **Abele, R. and Tampé, R.,** Moving the cellular peptidome by transporters. *Front. Cell Dev. Biol.* 2018. **6**: 43.

7 **Thomas, C. and Tampe, R.,** MHC I chaperone complexes shaping immunity. *Curr. Opin. Immunol.* 2019. **58**: 9–15.

8 **Madden, D. R.,** The three-dimensional structure of peptide-MHC complexes. *Annu. Rev. Immunol.* 1995. **13**: 587–622.

9 **York, I. A., Chang, S.-C. C., Saric, T., Keys, J. A., Favreau, J. M., Goldberg, A. L. and Rock, K. L.,** The ER aminopeptidase ERAP1 enhances or limits antigen presentation by trimming epitopes to 8–9 residues. *Nat. Immunol.* 2002. **3**: 1177–1184.

10 **Lopez de Castro, J. A.,** How ERAP1 and ERAP2 shape the peptidomes of disease-associated MHC-I proteins. *Front. Immunol.* 2018. **9**: 2463.

11 **Stratikos, E., Stamogiannos, A., Zervoudi, E. and Fruci, D.,** A role for naturally occurring alleles of endoplasmic reticulum aminopeptidases in tumor immunity and cancer pre-disposition. *Front. Oncol.* 2014. **4**: 363.

12 **Mpakali, A., Maben, Z., Stern, L. J. and Stratikos, E.,** Molecular pathways for antigenic peptide generation by ER aminopeptidase 1. *Mol. Immunol.* 2019. **113**: 50–57.

13 **Hutchinson, J. P., Temponeras, I., Kuiper, J., Cortes, A., Korczynska, J., Kitchen, S. and Stratikos, E.,** Common allotypes of ER aminopeptidase 1 have substrate-dependent and highly variable enzymatic properties. *J. Biol. Chem.* 2021. **296**: 100443.

14 **Stamatakis, G., Samiotaki, M., Temponeras, I., Panayotou, G. and Stratikos, E.,** Allotypic variation in antigen processing controls antigenic peptide generation from SARS-CoV-2 S1 spike glycoprotein. *J. Biol. Chem.* 2021. **297**: 101329.

15 **Stratikos, E.,** Regulating adaptive immune responses using small molecule modulators of aminopeptidases that process antigenic peptides. *Curr. Opin. Chem. Biol.* 2014. **23**: 1–7.

16 **Reeves, E., Islam, Y. and James, E.,** ERAP1: A potential therapeutic target for a myriad of diseases. *Expert Opin. Ther. Targets* 2020. **24**: 535–544.

17 **Georgiadis, D., Mpakali, A., Koumantou, D. and Stratikos, E.,** Inhibitors of ER aminopeptidase 1 and 2: from design to clinical application. *Curr. Med. Chem.* 2019. **26**: 2715–2729.

18 **Liddle, J., Hutchinson, J. P., Kitchen, S., Rowland, P., Neu, M., Cecconie, T., Holmes, D. S. et al.,** Targeting the regulatory site of ER aminopeptidase 1 leads to the discovery of a natural product modulator of antigen presentation. *J. Med. Chem.* 2020. **63**: 3348–3358.

19 **Maben, Z., Arya, R., Rane, D., An, W. F., Metkar, S., Hickey, M., Bender, S. et al.**, Discovery of selective inhibitors of endoplasmic reticulum aminopeptidase 1. *J. Med. Chem.* 2020. **63**: 103–121.

20 **Deddouche-Grass, S., Andouche, C., Bärenz, F., Halter, C., Hohwald, A., Lebrun, L., Membré, N. et al.**, Discovery and optimization of a series of benzofuran selective ERAP1 inhibitors: biochemical and in silico studies. *ACS Med. Chem. Lett.* 2021. **12**: 1137–1142.

21 **Joyce, P., Quibell, M., Shiers, J., Tong, C., Clark, K., Ternette, N., Anderton, K. et al.**, 553 First-in-class inhibitors of ERAP1 alter the immunopeptidome of cancer, driving a differentiated T cell response leading to tumor growth inhibition. *J. Immunother. Cancer* 2021. **9**(Suppl): A583.

22 **Papakyriakou, A. and Stratikos, E.**, The role of conformational dynamics in antigen trimming by intracellular aminopeptidases. *Front. Immunol.* 2017. **8**: 946.

23 **Nguyen, T. T., Chang, S.-C., Evnouchidou, I., York, I. A., Zikos, C., Rock, K. L., Goldberg, A. L. et al.**, Structural basis for antigenic peptide precursor processing by the endoplasmic reticulum aminopeptidase ERAP1. *Nat. Struct. Mol. Biol.* 2011. **18**: 604–613.

24 **Kochan, G., Krojer, T., Harvey, D., Fischer, R., Chen, L., Vollmar, M., von Delft, F. et al.**, Crystal structures of the endoplasmic reticulum aminopeptidase-1 (ERAP1) reveal the molecular basis for *N*-terminal peptide trimming. *Proc. Natl. Acad. Sci. U. S. A.* 2011. **108**: 7745–7750.

25 **Maben, Z., Arya, R., Georgiadis, D., Stratikos, E. and Stern, L. J.**, Conformational dynamics linked to domain closure and substrate binding explain the ERAP1 allosteric regulation mechanism. *Nat. Commun.* 2021. **12**: 5302.

26 **Giastas, P., Mpakali, A., Papakyriakou, A., Lelis, A., Kokkala, P., Neu, M., Rowland, P. et al.**, Mechanism for antigenic peptide selection by endoplasmic reticulum aminopeptidase 1. *Proc. Natl. Acad. Sci. U. S. A.* 2019. **116**: 26709–26716.

27 **Bruderer, R., Bernhardt, O. M., Gandhi, T., Miladinović, S. M., Cheng, L.-Y., Messner, S., Ehrenberger, T. et al.**, Extending the limits of quantitative proteome profiling with data-independent acquisition and application to acetaminophen-treated three-dimensional liver microtissues. *Mol. Cell. Proteomics* 2015. **14**: 1400–1410.

28 **Alvarez-Navarro, C., Martín-Esteban, A., Barnea, E., Admon, A. and López De Castro, J. A.**, Endoplasmic reticulum aminopeptidase 1 (ERAP1) polymorphism relevant to inflammatory disease shapes the peptidome of the birdshot chorioretinopathy-associated HLA-A*29:02 antigen. *Mol. Cell. Proteomics* 2015. **14**: 1770–1780.

29 **Barnea, E., Melamed Kadosh, D., Haimovich, Y., Satumtira, N., Dorris, M. L., Nguyen, M. T., Hammer, R. E. et al.**, The human leukocyte antigen (HLA)-B27 peptidome in vivo, in spondyloarthritis-susceptible HLA-B27 transgenic rats and the effect of Erap1 deletion. *Mol. Cell. Proteomics* 2017. **16**: 642–662.

30 **Guasp, P., Barnea, E., Gonzalez-Escribano, M. F., Jimenez-Reinoso, A., Regueiro, J. R., Admon, A. and Lopez de Castro, J. A.**, The behcet's disease-associated variant of the aminopeptidase ERAP1 shapes a low-affinity HLA-B*51 peptidome by differential subpeptidome processing. *J. Biol. Chem.* 2017. **292**: 9680–9689.

31 **Patil, I.**, Visualizations with statistical details: The "ggstatsplot" approach. *J. Open Source Softw.* 2021. **6**: 3167.

32 **Sarkizova, S., Klaeger, S., Le, P. M., Li, L. W., Oliveira, G., Keshishian, H., Hartigan, C. R. et al.**, A large peptidome dataset improves HLA class I epitope prediction across most of the human population. *Nat. Biotechnol.* 2020. **38**: 199–209.

33 **Hammer, G. E., Gonzalez, F., James, E., Nolla, H. and Shastri, N.**, In the absence of aminopeptidase ERAAP, MHC class I molecules present many unstable and highly immunogenic peptides. *Nat. Immunol.* 2007. **8**: 101–108.

34 **Chong, C., Müller, M., Pak, H. S., Harnett, D., Huber, F., Grun, D., Leleu, M. et al.**, Integrated proteogenomic deep sequencing and analytics accurately identify non-canonical peptides in tumor immunopeptidomes. *Nat. Commun.* 2020. **11**, https://doi.org/10.1038/s41467-020-14968-9

35 **Evnouchidou, I., Momburg, F., Papakyriakou, A., Chroni, A., Leondiadis, L., Chang, S.-C., Goldberg, A. L. et al.**, The internal sequence of the peptide-substrate determines its n-terminus trimming by ERAP1. *PLoS One* 2008. **3**: e3658.

36 **Goslee, S. C. and Urban, D. L.**, The ecodist package for dissimilarity-based analysis of ecological data. *J. Stat. Softw.* 2007. **22**: 1–19.

37 **Zervoudi, E., Papakyriakou, A., Georgiadou, D., Evnouchidou, I., Gajda, A., Poreba, M., Salvesen, G. S. et al.**, Probing the S1 specificity pocket of the aminopeptidases that generate antigenic peptides. *Biochem. J.* 2011. **435**: 411–420.

38 **Ran, F. A., Hsu, P. D., Wright, J., Agarwala, V., Scott, D. A. and Zhang, F.**, Genome engineering using the CRISPR-Cas9 system. *Nat. Protoc.* 2013. **8**: 2281–2308.

39 **Temponeras, I., Stamatakis, G., Samiotaki, M., Georgiadis, D., Pratsinis, H., Panayotou, G. and Stratikos, E.**, ERAP2 inhibition induces cell-surface presentation by MOLT-4 leukemia cancer cells of many novel and potentially antigenic peptides. *Int. J. Mol. Sci.* 2022. **23**: 1913.

40 **Hughes, C. S., Moggridge, S., Müller, T., Sorensen, P. H., Morin, G. B. and Krijgsveld, J.**, Single-pot, solid-phase-enhanced sample preparation for proteomics experiments. *Nat. Protoc.* 2019. **14**: 68–85.

41 **Venema, W. J., Hiddingh, S., de Boer, J. H., Claas, F. H. J., Mulder, A., den Hollander, A. I., Stratikos, E. et al.**, ERAP2 increases the abundance of a peptide submotif highly selective for the birdshot uveitis-associated HLA-A29. *Front. Immunol.* 2021. **12**: 634441.

42 **Hennig, C.** Flexible procedures for clustering. 2020

43 **Hahsler, M., Piekenbrock, M. and Doran, D.**, Dbscan: fast density-based clustering with R. *J. Stat. Softw.* 2019. **91**: 1–30.

44 **Wagih, O. G.** A versatile R package for drawing sequence logos. *Bioinforma. Oxf. Engl.* 2017. **33**: 3645–3647.

45 **Stratikos, E.**, Modulating antigen processing for cancer immunotherapy. *Oncoimmunology* 2014. **3**: e27568.

46 **Schumacher, T. N. and Schreiber, R. D.**, Neoantigens in cancer immunotherapy. *Science* 2015. **348**: 69–74.

47 **McGonagle, D., Aydin, S. Z., Gul, A., Mahr, A. and Direskeneli, H.** 'MHC-I-Opathy'-unified concept for spondyloarthritis and behcet disease. *Nat. Rev. Rheumatol.* 2015. **11**: 731–740.

48 **Yang, X., Garner, L. I., Zvyagin, I. V., Paley, M. A., Komech, E. A., Jude, K. M., Zhao, X. et al.**, Autoimmunity-associated T cell receptors recognize HLA-B*27-bound peptides. *Nature* 2022. **612**: 771–777.

49 **Arakawa, A., Reeves, E., Vollmer, S., Arakawa, Y., He, M., Galinski, A., Stöhr, J. et al.**, ERAP1 controls the autoimmune response against melanocytes in psoriasis by generating the melanocyte autoantigen and regulating its amount for HLA-C*06:02 presentation. *J. Immunol. Baltim. Md. 1950* 2021. **207**: 2235–2244.

50 **James, E., Bailey, I., Sugiyarto, G. and Elliott, T.** Induction of protective antitumor immunity through attenuation of ERAAP function. *J. Immunol.* 2013. **190**: 5839–5846.

51 **Admon, A.**, ERAP1 shapes just part of the immunopeptidome. *Hum. Immunol.* 2019. **80**: 296–301.

52 **Hisatsune, C., Ebisui, E., Usui, M., Ogawa, N., Suzuki, A., Mataga, N., Takahashi-Iwanaga, H. et al.**, ERp44 exerts redox-dependent control of blood pressure at the ER. *Mol. Cell* 2015. **58**: 1015–1027.

53 **Saveanu, L., Carroll, O., Lindo, V., Del Val, M., Lopez, D., Lepelletier, Y., Greer, F. et al.**, Concerted peptide trimming by human ERAP1 and ERAP2 aminopeptidase complexes in the endoplasmic reticulum. *Nat. Immunol.* 2005. **6**: 689–697.

54 **Papakyriakou, A., Mpakali, A. and Stratikos, E.**, Can ERAP1 and ERAP2 form functional heterodimers? A structural dynamics investigation. *Front. Immunol.* 2022. **13**: 863529.

55 **Aldhamen, Y. A., Pepelyayeva, Y., Rastall, D. P. W., Seregin, S. S., Zervoudi, E., Koumantou, D., Aylsworth, C. F. et al.**, Autoimmune disease-associated variants of extracellular endoplasmic reticulum aminopeptidase 1 induce altered innate immune responses by human immune cells. *J. Innate Immun.* 2015. **7**: 275–289.

56 **Schmidt, K., Leisegang, M. and Kloetzel, P.-M.**, ERAP2 supports TCR recognition of three immunotherapy targeted tumor epitopes. *Mol. Immunol.* 2023. **154**: 61–68.

57 **Perez-Riverol, Y., Csordas, A., Bai, J., Bernal-Llinares, M., Hewapathirana, S., Kundu, D. J., Inuganti, A. et al.**, The PRIDE database and related tools and resources in 2019: Improving support for quantification data. *Nucleic. Acids. Res.* 2019. **47**: D442–D450.

Abbreviations: **ATCC:** American Type Culture Collection · **AGC:** automated gain control · **ERAP1:** ER aminopeptidase 1 · **NMDS:** nonmetric multidimensional scaling

Full correspondence: Dr. Efstratios Stratikos, National Centre for Scientific Research Demokritos, Agia Paraskevi, Greece.
e-mail: estratikos@chem.uoa.gr